ELSEVIER

Synthetic Metals 103 (1999) 1925–1928

SYNTHETIC METALS

Stability of the vortex lattice in ET superconductors studied by μSR

S.J. Blundell[1], S.L. Lee[2], F.L. Pratt[1,3], C.M. Aegerter[4], Th. Jestädt[1], B.W. Lovett[1], C. Ager[2], T.Sasaki[5], V.N. Laukhin[6], E. Laukhina[7], E.M. Forgan[8], and W.Hayes[1]

[1] *Clarendon Laboratory, Oxford University Department of Physics, Parks Road, Oxford, OX1 3PU, United Kingdom*
[2] *School of Physics and Astronomy, University of St. Andrews, St. Andrews, Fife KY16 9SS, United Kingdom*
[3] *RIKEN-RAL, Chilton, Didcot, Oxon OX11 0QX, United Kingdom*
[4] *Physik-Institut, Universität Zürich, CH-8057 Zürich, Switzerland*
[5] *Institute for Materials Research, Tohoku University, Sendai 980-77, Japan*
[6] *Institut de Ciéncia de Materials de Barcelona (CSIC), Campus UAB, E-08193 Bellaterra, Spain*
[7] *Institute of Chemical Physics, Russian Academy of Sciences, Chernogolovka 142432, Russia*
[8] *School of Physics and Space Research, University of Birmingham, Birmingham B15 2TT, United Kingdom*

Abstract

Muon-spin rotation (μSR) measurements have been used to study the vortex lattice and its instabilities in the organic superconductors κ-$ET_2Cu(SCN)_2$ and β-ET_2IBr_2. We ascribe the field- and temperature-dependent destruction of the vortex lattice to the large anisotropy found in these materials.

Keywords: Organic superconductors, magnetic measurements, muon spin rotation, superconducting phase transitions, nuclear magnetic resonance spectroscopy.

1. Introduction

Layered organic superconductors based on the molecule ET (bis(ethylenedithio)tetrathiafulvalene, also known as BEDT-TTF) share a distinctive property of many cuprate superconductors, namely that they are extremely anisotropic. This leads to highly unconventional behaviour in the B–T phase-diagram [1]. A conventional type II superconductor exhibits 3 well-defined phases for $T < T_c$: (1) a Meissner phase for $B < B_{c1}$, (2) a mixed or Shubnikov phase for $B_{c1} < B < B_{c2}$ (in which the magnetic field enters the superconductor in the form of well defined flux lines or vortices arranged in an Abrikosov lattice) and (3) the normal metallic phase for $B > B_{c2}$.

In highly anisotropic systems the vortex lattice is no longer a system of rigid rods but should be considered as a system of flexible interacting lines. A useful picture is that of a weakly coupled stack of quasi-two-dimensional (q2D) "pancake" vortices, each one confined to a superconducting plane [1–3]. The phase diagram is thus substantially altered to take account of field and temperature dependent changes in the vortex lattice itself. At low T and low B the stacks resemble conventional vortex lines. Above a characteristic temperature T_b, but still below that at which superconductivity is destroyed, the vortex lattice is broken up by thermal fluctuations [2] (vortex lattice melting). At low T but this time increasing B the energetic cost of interlayer deformations of the lattice (local tilting of the lines) is progressively outweighed by the cost of intralayer deformations within the superconducting plane (shearing). Above a crossover field B_{cr} the vortex lattice enters a more two-dimensional regime [3,4]. Thus in anisotropic systems we may expect temperature and field dependent transitions in which the vortex lattice is destroyed.

2. μSR and superconductors

The two important lengthscales in superconductors are the penetration depth, λ, and the coherence length, ξ. If $\lambda > \xi/\sqrt{2}$ we have a type II superconductor which if cooled through T_c in an applied magnetic field remains superconducting everywhere except in a triangular lattice of vortex cores. Each vortex is associated with a magnetic flux equal to one flux quantum $\phi_0 = h/2e$. The distance between vortices, d, is such that the number of vortices per unit area $2/\sqrt{3}d^2$ equals the number of flux quanta per unit area B/ϕ_0. Thus $d \propto B^{-1/2}$. In general the vortex lattice will be incommensurate with the crystal lattice and d will be much larger than the crystal lattice constant a. Implanted muons sit at certain crystallographic sites and thus randomly sample the field distribution of the vortex lattice.

In the normal state ($T > T_c$) with a transverse field B, all muons precess with angular frequency $\omega = \gamma_\mu B$

PII: S0379-6779(98)00349-X

where γ_μ is the muonic gyromagnetic ratio. In the superconducting state the muons implanted close to the vortex cores experience a larger magnetic field than those implanted between vortices. Consequently there is a spread in precession frequency, resulting in a progressive dephasing of the observed precession signal. The larger the penetration depth, the smaller the magnetic field variation and the less pronounced the dephasing. Thus the relaxation rate σ of the observed precession signal can be used to directly infer the magnetic penetration depth [5,6] using

$$\sigma = \gamma_\mu \langle B(\mathbf{r}) - \langle B(\mathbf{r})\rangle_\mathbf{r}\rangle_\mathbf{r}^{1/2} \approx 0.0609\gamma_\mu \Phi_0/\lambda^2. \quad (1)$$

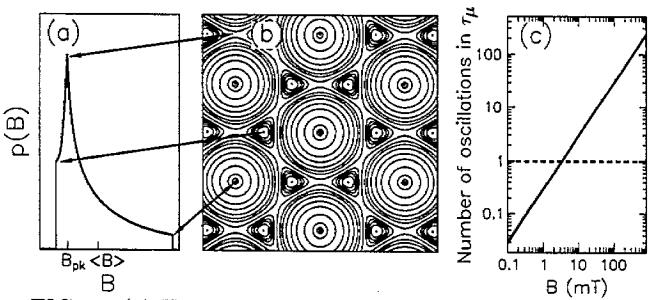

FIG. 1. (a) The field distribution $p(B)$ in the vortex lattice (contours of B shown in (b)). (c) The number of muon-spin precessions that can occur in a muon lifetime τ_μ =2.2 μs for different transverse magnetic fields.

μSR experiments have been particularly useful in studies on organic metals, conductors and magnets [7]. When applied to a superconductor in a field B one can directly measure the field distribution $p(B')$ which is given by $p(B') = \langle\delta(B' - B(\mathbf{r}))\rangle_\mathbf{r}$ and is the probability that a randomly chosen point in the sample has field B' [6,8]. This is shown in Fig. 1(a) for an ideal vortex line lattice. The distribution is highly asymmetric, the high field "tail" corresponding to regions of the lattice close to the vortex cores (see Fig. 1(b)). The maximum of the distribution occurs at B_{pk}, which lies below the mean field $\langle B\rangle$ (see Fig. 1(a)). Such lineshapes have been observed in the high temperature superconductors using μSR [8]. It is easier to make such measurements at high magnetic fields because a larger number of precessions can be observed during the muon lifetime (see Fig. 1(c)).

3. Experimental

Muons, which are approximately 100 % spin polarized anti-parallel to their momentum ($\approx$ 29 MeV/c), are implanted into a mosaic of high-quality single crystals grown by an electrochemical oxidation. The individual crystals are platelets of typical dimensions 1.0×1.5×0.5 mm^3 with the largest face parallel to the superconducting planes ($\hat{b}$-$\hat{c}$ planes). The crystals were mounted with Apiezon grease on a plate of haematite (Fe_2O_3) to give a total area approximately 10×20 mm^2. The use of a haematite backing plate ensures that any muons not stopping in the sample are rapidly depolarized outside of the μSR time window, so that the resulting spectra contain information relating only to the sample. The experiments were conducted in the transverse-field geometry where the initial muon spin is perpendicular to the applied magnetic field. In most experiments the sample was arranged so that the superconducting planes made an angle of 45° with both the field and with the muon momentum. μSR experiments were carried out at the ISIS facility at the Rutherford Appleton Laboratory, U.K., which provides pulsed beams of positive muons at a frequency of 50 Hz with a width of $\approx$ 70 ns. The polarization of the muons at ISIS cannot be rotated, so this geometry was chosen to provide a reasonable cross-sectional area of sample to the beam, while also allowing the field to be directed at a large angle to the superconducting planes. Further experiments were performed using the continuous muon beam at the Paul Scherrer Institute (PSI) in Switzerland which possesses a spin rotator. Angle-dependence was therefore measured by using data from ISIS together with that obtained at PSI in which the experimental configuration is complementary.

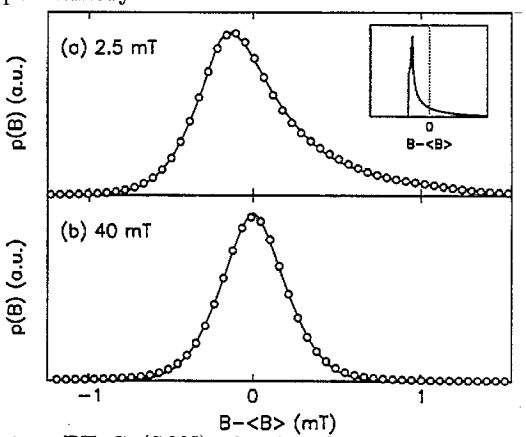

FIG. 2. κ-$ET_2Cu(SCN)_2$ showing the measured lineshape when field cooled to 1.8 K in a field applied at 45° to the superconducting planes. (a) At 2.5 mT the characteristic asymmetric vortex-line-lattice shape is seen. [Note the circles are data, solid line is simulation of ideal vortex-line-shape convoluted with instrument response. The inset shows the computed $p(B)$ before convolution.] (b) At 40 mT a symmetric line-shape is obtained due to the 2D arrangement of pancake vortices which results in a more symmetrical vortex field distribution.

4. Results

The superconductor κ-$ET_2Cu(SCN)_2$ has a transition temperature of 10.4 K, making it one of the highest-temperature organic superconductors and has a Fermi surface which is characterised by a quasi-2D Fermi surface topology [9]. Recent *ac*-susceptibility mea-

surements yielded an estimate of the superconducting anisotropy parameter $\gamma = \lambda_\perp/\lambda_{||} \approx 160 - 350$, where $\lambda_\perp$ ($\lambda_{||}$) are the superconducting penetration depths for currents flowing perpendicular (parallel) to the superconducting planes in a uniaxial system [10].

Figure 2(a) is a μSR lineshape measured at 1.8 K for a sample cooled in a field of 2.5 mT, which was derived from the muon time spectra using a maximum entropy technique [8,11]. The inset curve in Figure 2(a) is the probability distribution $p(B)$ from a numerical simulation of a vortex-line lattice in a uniaxial superconductor at an angle of 45° to the superconducting planes. The solid curve in the main part of Fig. 2(a) is the convolution of this field distribution with instrumental and dipolar broadening of 0.23 mT, which describes the data well. The long penetration depth in ET superconductors means that the lineshape is very narrow and the dipolar broadening very significant. Moreover the very low field used to ensure the existence of the vortex lattice means that it is essential to use a pulsed muon source such as ISIS since the very long time window available reduces the contribution from instrumental broadening.

Figure 2(b) shows the μSR-lineshape taken for the same sample cooled in a larger field of 40 mT. The results in this case are very similar to previously published lineshapes in κ-$ET_2Cu(SCN)_2$ [12–14] which were all performed at high field. The lineshape is highly symmetric, with a mode at B_{pk} close to the average field $\langle B \rangle$. This change of lineshape with field is very similar to changes observed in the high-T_c superconductor $Bi_2Sr_2CaCu_2O_{8+\delta}$ (BSCCO), and indicates the loss of short-range correlations of the pancake vortices along the field direction [8]. It is attributed to the effective smearing-out of the core fields due to the local tilt deformations of the pancake stacks [8,15].

Previous studies of κ-$ET_2Cu(SCN)_2$ using μSR have concentrated mainly on determining the value and temperature dependence of the in-plane superconducting penetration depth $\lambda_{||}(T)$ [12–14] in order to deduce strength and symmetry of the superconducting pairing but have obtained contradictory results. Our results demonstrate the existence in κ-$ET_2Cu(SCN)_2$ of a flux-line lattice only at low fields. At the higher fields used in previous studies the probability distributions indicate only q2D order, with reduced correlations of vortex segments along the field direction, so that as suggested by Lang *et al.* the discrepancies between earlier μSR measurements can be due to the metastability of the vortex lattice [16]. At low field we accurately measure the penetration depth for the first time and obtain a value of $\lambda_{||} = 538(8)$ nm [17,18] in good agreement with the value obtained from reversible magnetization $\lambda_{||} = 535(20)$ nm [19].

We quantify the lineshape by a dimensionless skewness parameter, β, appropriate for the very narrow lineshapes which occur in κ-$ET_2Cu(SCN)_2$, which we define as $\beta = (\langle B \rangle - B_{pk}) / \left(\langle B^2 \rangle - \langle B \rangle^2\right)^{1/2}$. A value of $\beta = 0$ indicates a symmetric lineshape, while a positive value reflects a weighting toward fields higher than B_{pk}, as is the case for a lineshape arising from a vortex line lattice (Fig. 2(a)). As a function of field we find that there is a broad crossover centred around $B_{cr} \sim 7$ mT from the asymmetric lineshape of Fig. 2(a) to the almost symmetric lineshape of Fig. 2(b) [17].

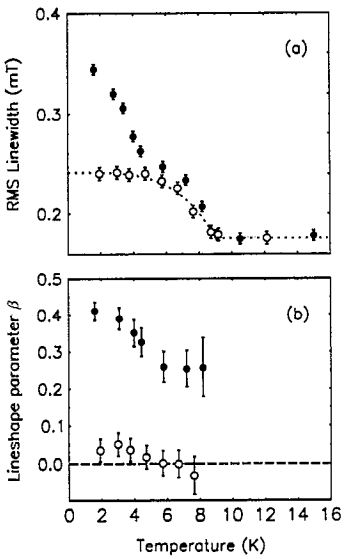

FIG. 3. (a) The temperature dependence of the total μSR linewidth for applied fields of 2.5 mT (solid circles) and 30 mT (empty circles). At 30 mT, which is above B_{cr}, the temperature dependence is consistent with a two-fluid-like dependence of λ (dashed line) with the narrow linewidth expected for a quasi-2D flux arrangment. For 2.5 mT, which is below B_{cr} , the lineshape rapidly becomes narrower between 3 and 5 K and above 5 K it follows a similar dependence to that seen above B_{cr}. (b) At 2.5 mT (solid circles) the narrowing of the linewidth is accompanied by a significant fall in β, centred around a crossover temperature $T^* \sim 5$ K, which indicates a reduction of pancake vortex correlations along the field direction above T^*.

For a rigid vortex-line lattice the temperature dependence of the linewidth $\langle \Delta B^2 \rangle^{1/2}(T) \propto 1/\lambda^2$, where λ is the effective penetration depth in a plane perpendicular to the applied field. However, for unconventional flexible or quasi-2D lattices the $\langle \Delta B^2 \rangle^{1/2}(T)$ may be influenced by other temperature-dependent effects on the lattice structure, such as thermally induced fluctuations and vortex-lattice melting.

Figure 3(a) shows the linewidth $\langle \Delta B^2 \rangle^{1/2}(T)$ for fields above and below B_{cr}. For $B > B_{cr}$, the linewidth is very narrow and β is close to zero (Fig. 3(b)); $\langle \Delta B^2 \rangle^{1/2}(T)$ is not inconsistent with that expected for a conventional *s*-wave superconductor, as also found in ref. [14]. However, for $B < B_{cr}$ there is a dramatic increase in linewidth below $T^* \sim 5$ K. More signifi-

cantly, Fig. 3(b) shows that the *lineshape* also changes around T^*. While for $T < T^*$ the value of β approaches that expected for an ideal vortex-line lattice, this value falls rapidly with T and plateaus at a significantly reduced value. This reduction in β, reflecting a change in line*shape*, indicates a reduction of pancake vortex correlations along the field direction. An estimate of the characteristic temperature for the thermally-induced breakup of an electromagnetically-coupled pancake stack is given by $T_b = \phi_0^2 s/k_B\mu_0(4\pi)^2 2\lambda_{||}^2 \approx 4.5$ K [2] where s is the interlayer spacing. The reduction in the positional correlations of pancake vortices at $T^* \sim 5$K is thus consistent with this prediction [17].

The crossover field B_{cr} is closely related to the "second-peak" effect which has been observed in magnetization hysteresis loops [20]. For a Josephson coupled superconductor ($\lambda_{||} \gg \gamma s$) the dimensional crossover is expected at a field $B_J \sim \phi_o/(\gamma s)^2$ when the width of the Josephson vortex core γs equals the vortex separation. When the anisotropy is very large $\gamma s \gg \lambda_{||}$ the rigidity of the vortex line is controlled by the tilt modulus of the lattice and is dominated by a highly dispersive electromagnetic interaction so that despite long wavelength stiffness the vortices are subject to short wavelength fluctuations [4,22]. Electromagnetic coupling is believed to dominate in BSCCO [21,22] and κ-$ET_2Cu(SCN)_2$ [17] and taking the layer separation for κ-$ET_2Cu(SCN)_2$ as $s \sim 1.6$ nm yields an estimate $B_{cr} \sim 7$mT which is in agreement with our experiment [17].

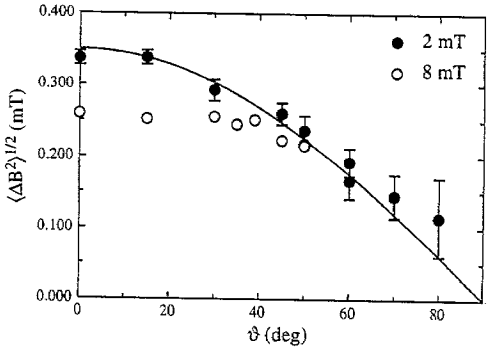

FIG. 4. κ-$ET_2Cu(SCN)_2$ linewidth as a function of angle.

Further confirmation of the presence of a vortex line lattice can be obtained from angle-dependent measurements (for analogous measurements in BSCCO see [11]) (Fig. 4). The linewidth as a function of angle is given by

$$\langle \Delta B^2 \rangle^{1/2}(\theta) = \langle \Delta B^2 \rangle^{1/2}(0)[cos^2\theta + \gamma^{-2}\sin^2\theta]^{1/2}, \quad (2)$$

which gives a $\cos\theta$ dependence when $\gamma \gg 1$, as observed when B =2 mT. This begins to break down when B =8 mT since in this case $B > B_{cr}$.

We are currently extending this technique to other ET superconductors. which have different crystal structures, different anisotropies and different superconducting transition temperatures. This allows one to vary different energy scales in the vortex lattice and test theoretical predictions of the consequent magnetic phase diagram and associated break-up temperatures and crossover fields. Although the *thermal* energy available for vortex disruption is much less than in high-T_c superconductors, the vortices are much more susceptible to fluctuations due to the large anisotropy and Ginzburg Landau parameter, and hence these are systems which really can show melting behaviour at low temperatures. Preliminary results on β''-ET_2IBr_2 (Fig. 5) show similar behaviour to κ-$ET_2Cu(SCN)_2$ with a possible T^* at 1.5 K.

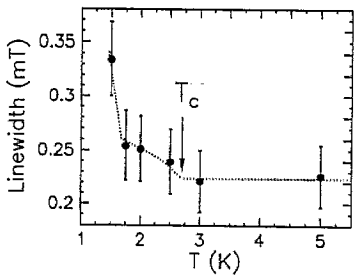

FIG. 5. Linewidth in β''-ET_2IBr_2 in a magnetic field of 1 mT. The line is a guide to the eye.

We would like to thank the staff of the ISIS and PSI muon facilities for their assistance. We also acknowledge the financial support of the EPSRC of the United Kingdom and the Swiss National Science Foundation.

REFERENCES

[1] G. Blatter *et al.* Rev. Mod. Phys. **66**, 1125 (1995).
[2] J.R. Clem Phys. Rev. B **43**, 7837 (1991).
[3] L.I. Glazman *et al.* Phys. Rev. B **43**, 2835 (1991).
[4] G. Blatter *et al.* Phys. Rev. B **54**, 72 (1996).
[5] E.H. Brandt and A. Seeger Adv. Phys. **35**, 189 (1986).
[6] E.H. Brandt Phys. Rev. B **37**, 2349 (1988).
[7] S.J. Blundell Appl. Mag. Res. **13**, 155 (1997)
[8] C.M. Aegerter and S.L. Lee Appl. Mag. Res. **13**, 75 (1997); S.L. Lee *et al.* Phys. Rev. Lett. **71**, 3862 (1993); Phys. Rev. Lett. **75**, 922 (1995).
[9] Organic Superconductors, by T. Ishiguro and K. Yamaji, (Springer-Velag, Berlin 1990).
[10] P. A. Mansky *et al.* Phys. Rev. B **50**, 15929 (1994).
[11] C.M. Aegerter *et al.* Phys. Rev. B **57**, 1253 (1998).
[12] D.R. Harshman *et al.* Phys. Rev. Lett. **64**, 1293 (1990).
[13] L.P. Le *et al.* Phys. Rev. Lett. **68**, 1923 (1992).
[14] D.R. Harshman *et al.* Phys. Rev. B **49**, 12990 (1994).
[15] E.H. Brandt Phys. Rev. Lett. **66**, 3213 (1991); J. Low Temp. Phys. **73**, 355 (1988).
[16] M. Lang *et al.* Phys. Rev. B **49**, 15227 (1994).
[17] S.L. Lee *et al. Phys. Rev. Lett.* **79**, 1563 (1997)
[18] S.L. Lee *et al. Synth. Met.* **85**, 1495 (1997)
[19] M. Lang *et al.* Phys. Rev. Lett. **63**, 1106 (1989).
[20] T. Nishizaki *et al.* Phys. Rev. B **54**, R3670 (1996).
[21] C.M. Aegerter *et al.* Phys. Rev. B **54**, R15661 (1996).
[22] S.L. Lee *et al.* Phys. Rev. B **55**, 5666 (1997).